



ELSEVIER

Coastal Engineering 41 (2000) 317–352

**COASTAL  
ENGINEERING**

www.elsevier.com/locate/coastaleng

## Suspended sediment modelling in a shelf sea (North Sea)

Herman Gerritsen<sup>a,\*</sup>, Robert J. Vos<sup>a,1</sup>, Theo van der Kaaij<sup>a</sup>,  
Andrew Lane<sup>b</sup>, Johan G. Boon<sup>a</sup>

<sup>a</sup> WL/Delft Hydraulics, P.O. Box 177, 2600 MH Delft, Netherlands

<sup>b</sup> Proudman Oceanographic Laboratory, Bidston Observatory, Birkenhead, CH43 7RA, UK

---

### Abstract

This paper extends the modelling of suspended particulate matter (SPM) on the local coastal scale (described in preceding papers) to SPM modelling on the scale of the North Sea, focusing on representing SPM patterns and their seasonal distribution. The modelling includes a sensitivity study, in which model results are assessed using surface SPM concentration patterns extracted from NOAA reflectance imagery, as well as North Sea Project in situ data.

Over the past decade or so, first-order estimates of the net suspended load and its associated sources and sinks have been available and are generally substantiated. However, developments in the simulation of large-scale SPM behaviour are still severely restricted by the available descriptions of available sediment sources and sediment erosion and deposition processes. This paper indicates how remotely sensed reflectance images can provide additional information on the spatial distribution of (sea surface) suspended sediments.

A primary objective of this paper is to examine sensitivities of SPM simulations in 2D (vertically averaged) and 3D models. A boundary-fitted coordinate modelling approach with intra-tidal resolution and synoptic meteorology is applied, as well as more schematic approaches. A related objective is to examine how both limited in situ observational data and reflectance imagery can be used to assess and improve such simulations.

An integrated modelling-monitoring approach, using inverse and ‘Goodness-of-Fit’ (GoF) approaches applied to remotely sensed reflectance imagery, is used to derive a structured sensitivity analysis providing a quantified assessment of the strengths and weaknesses of modelling and input data. It is shown that, especially in the coastal zone where salinity stratification

---

\* Corresponding author. Tel.: +31-15-2858470; fax: +31-15-285-8582.

E-mail address: herman.gerritsen@wldelft.nl (H. Gerritsen).

<sup>1</sup> Present address: University of Amsterdam, Institute for Environmental Studies, de Boelelaan 1105, 1081 HV Amsterdam, Netherlands.

may occur, 3D modelling is required while much of the sensitivity analysis can be based on a 2D modelling approach. This quantification of the effects of uncertainties of inputs and erosion/deposition parameters improves understanding of the sediment distribution and budgets on the North Sea scale.

It is concluded that whilst process studies are likely to contribute to improving erosion/deposition algorithms, and model developments will provide enhanced dynamical descriptions, accurate overall simulation will remain dependent on some (inverse) processes to reduce the uncertainty in sediment sources. © 2000 Elsevier Science B.V. All rights reserved.

*Keywords:* Boundary-fitted modelling grid; NOAA/AVHRR reflectance imagery; Sensitivity analysis; Suspended sediment modelling; North Sea

---

## **1. Introduction**

A primary objective of PRE-Operational Modelling In the Seas of Europe (PROMISE) was to develop the methodology to ‘quantify the rates and scales of exchange of sediments between the coast and the near-shore zone’. This involves developing the capabilities to simulate near-shore waves (Monbalieu et al., 2000), couple these with currents (Ozer et al., 2000) and compute the resultant turbulence distributions (Baumert et al., 2000). While these models provide the dynamical framework for the suspended particulate matter (SPM) modelling, additional information on coastal and offshore sources of sediments is required — direct monitoring by remote sensing (Johannessen et al., 2000) or in situ observations (Lane et al., 2000) provide (by inverse means) such information. For eroding coasts, local area models (Prandle et al., 2000) can provide SPM input to shelf sea scale simulations. For other coastal zones (Schneeggenburger et al., 2000), SPM exchanges may constitute alternatively imports and exports — differing over seasons, tranquil or storm conditions and for fine-to-coarse sediments. In tidal straits (Chapalain and Thais, 2000), the exchange may be essentially a through-flow.

The primary objective of the modelling in this paper is the representation of the suspended sediment distribution or patterns on the scale of the North Sea and their variation over the seasons. A related objective is to perform structured sensitivity analyses to identify strengths and weaknesses of various approaches. The limited mobility of coarse, sandy sediments restricts consideration here to finer silt/clay particles, which can remain in suspension for periods of months. Both 2D and 3D approaches are considered. Tide resolving simulations with synoptic meteorology are made, as well as simulations with spatially and temporally averaged hydrodynamics and forcing. A novel feature is the use of a boundary-fitted coordinate grid with high resolution in the coastal zones alongside modelling on a rectangular grid. For validation of the model results, both SPM in situ data sets and newly available remotely sensed reflectance imagery are used.

Summarising the above, we re-examine our knowledge of larger-scale SPM budgets for the North Sea, with the aim of identifying how modelling developments in PROMISE and more traditional in situ data sets plus newly available remotely sensed data can be combined (Vos et al., 2000) to advance this knowledge. In terms of the

scales of interest, the present work is comparable to the work by Lehmann et al. (1995), i.e. essentially North Sea wide, while most other North Sea applications consider a small-scale local application (see e.g. de Kok, 1992).

Section 2 comprises a review of existing sediment budget estimates for the North Sea. Section 3 analyses the component modules required in a North Sea SPM model. Section 4 presents a 2D-model approach to determine the significance of sediment sources for the SPM distribution in the North Sea, using multiple linear regression (McManus and Prandle, 1997). Section 5 presents a sensitivity analysis of modelling of the North Sea SPM distribution and its seasonal distribution using a curvilinear grid in 2D and 3D and NOAA satellite reflectance imagery (see also Gerritsen et al., 2000). In the present analysis, attention is given to aspects such as uncertainties in hydrodynamics, forcing, etc., as well as SPM modelling per se.

Reiterating — the aim in the modelling simulation is to reproduce the North Sea scale SPM patterns and their seasonal variations — not individual localised, short-lived events. Given the synoptic nature of remote sensing imagery, these data are better suited for validation than much of the in situ data. Fig. 1 gives a characteristic composite

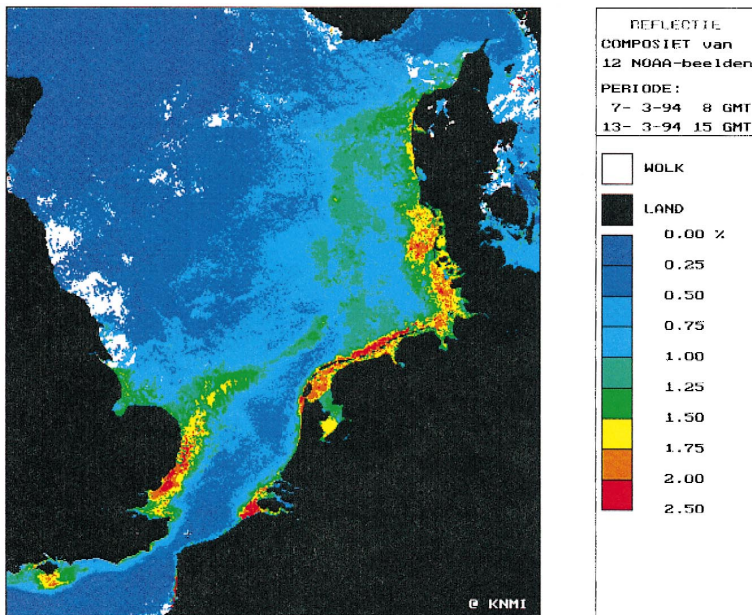


Fig. 1. North Sea remote sensing reflectance image for March 1994 (courtesy of KNMI). Note the plume of sediment across the North Sea. The continental coast features a high concentration of sediment in a rather narrow band of about 10–20 km.

reflectance image of the North Sea, which is a measure for the SPM distribution at the surface.

Conclusions and recommendations relating to future efforts follow in Section 6.

## 2. Estimation of North Sea SPM supplies and losses

Estimates of supply and loss of sediment for the entire North Sea (extending from the Dover Strait to the Atlantic Ocean and the Baltic Sea), obtained from several references in the literature are given in Appendix A, Tables A1 and A2. Many of these estimates show large uncertainties, and hence a detailed quantitative judgement may be misleading (Eisma and Irion, 1988). Estimates are given here as an indication of sources and sinks of SPM in the North Sea.

The tables show that the most relevant sources of sediment in the North Sea are in decreasing order of importance:

- An influx of  $20\text{--}40 \times 10^9 \text{ kg year}^{-1}$  through the Dover Strait
- Effect of dumping from dredging activities, estimated to be  $14 \times 10^9 \text{ kg year}^{-1}$
- Influx from the Atlantic Ocean of  $10 \times 10^9 \text{ kg year}^{-1}$
- Effect of coastal erosion from the east coast of England ( $2\text{--}8 \times 10^9 \text{ kg year}^{-1}$ )
- River inputs ( $4 \times 10^9 \text{ kg year}^{-1}$ )

Estimates of sediment losses are:

- Net sedimentation of  $32\text{--}45 \times 10^9 \text{ kg year}^{-1}$  (of which  $25 \times 10^9 \text{ kg year}^{-1}$  outside the model domain considered below)
- Net outflow to the Atlantic Ocean of  $11\text{--}14 \times 10^9 \text{ kg year}^{-1}$

## 3. SPM modelling — component specifications

SPM is usually defined as the particles in suspension with a diameter smaller than  $63 \mu\text{m}$  but may include all particles that are in suspension. In the North Sea Project (NSP) (Natural Environment Research Council, 1992), SPM was measured optically. In the North Sea, SPM determined with remote sensing usually corresponds to fine silt/clay, since only the top of the water column is sampled (phytoplankton can generally be differentiated in such data).

The SPM concentration is the result of the following three ‘processes’:

- Emissions of suspended matter (river discharges, sewage sludge, dumping and exchange with external waters (inputs and boundary conditions))
- Vertical transport and exchange with the seabed due to sedimentation and erosion processes, generated by currents and wind-induced waves
- Horizontal transport brought about by wind-, tide- and density-induced currents

So, to model the behaviour of North Sea suspended sediments and their seasonal variations, the following is required:

1. An accurate description of the (residual) flow field, characterised primarily by the volume flux through the Dover Strait, and accurate boundary conditions for the SPM concentration or SPM flux at the northern (upstream) model boundary.
2. Application of varying meteorological forcing using realistic (historic) wind data.
3. An assessment of the importance of stratification effects.
4. Inputs from dumping sites and rivers.
5. Accurately modelled sedimentation processes. Several size fractions of sediment may be required, stratification must be modelled and flocculation must probably be modelled.
6. Accurately modelled erosion. This may imply suitable initialisation of the bed surface sediment distribution in the model. Intra-tidally varying tide and wind–wave data may be required for modelling bed shear stress correctly.
7. Estimates of coastal erosion using literature budget estimates (McCave, 1987; Odd and Murphy, 1992; McManus and Prandle, 1997). Seasonal variation, e.g. the dependence on wind speed may be required (Vos and Schuttelaar, 1995).

The present sensitivity study to determine the effect of uncertainties in the inputs, forcing and model characteristics on the resulting concentrations and mass balance is essential to establish internal consistency and most realistic model prescriptions. The progressive increase in importance of wind–wave effects on SPM distributions in shallow water is emphasised elsewhere in this volume. The potential to dynamically couple such near-shore processes with larger-scale tidal and surge-dominated regimes further offshore is described in Ozer et al. (2000). Here, many such ‘sub-grid scale’ processes are neglected.

Three aspects require some further discussion.

### *3.1. The influence of meteorology*

Two important processes affecting sedimentation and erosion in the North Sea are tide and wind (the latter generates both currents and waves). Storm periods can be of significance for enhancing erosion and resuspension, but since these last at most a few days, it is not directly evident that they have a large effect on SPM fluxes for time scales of a few months. A typical time scale for SPM transport through the North Sea from Cap de La Hague to Denmark is about 1 year (Salomon et al., 1995). Periods with consistently high winds from one direction (usually southwest in the North Sea) are probably more important, since these significantly affect the SPM fluxes on longer time scales. Such periods are often found from December to March (i.e. during winter). SPM concentrations are much lower during summer (see Figs. 2 and 5 in Vos and Schuttelaar, 1995; Vos et al., 2000; Prandle et al., 1997; van Raaphorst et al., 1998). Although meteorology affects the transport of SPM significantly on a seasonal time scale, a highly

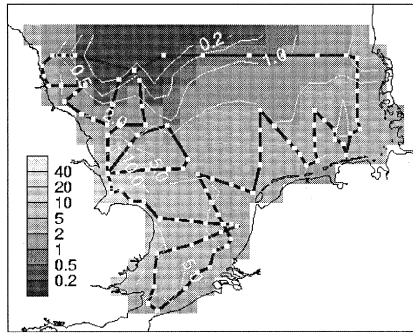


Fig. 2. Depth-averaged observed suspended sediment concentrations ( $\text{mg l}^{-1}$ ) during cruise CH47 (27/2–12/3/1989) of the North Sea Project. There were 15 such monthly surveys from August 1988 to October 1989. The ship's track is shown together with the sampling stations.

accurate description on an hourly basis is unnecessary for obtaining good estimates of SPM transport fluxes in the North Sea on the same time scale.

### 3.2. Stratification aspects

Stratification may have a significant effect on SPM concentrations in the upper part of the water column. For small particles, there is usually sufficient turbulent kinetic energy in the water column for a vertically homogeneous SPM distribution. However, stratified water particles will be trapped below the pycnocline, hence reducing the amount of SPM above it. In the North Sea, salinity stratification is expected in areas where river outflow is significant (Rhine and Elbe regions of freshwater influence). In thermally stratified waters (north of  $54^\circ\text{N}$ ), this effect is less important since the SPM concentration is generally low ( $< 2 \text{ mg l}^{-1}$ ).

### 3.3. Data aspects

Vos et al. (2000) show that the modelling objective is an important guide to setting up a model. This is especially true for an SPM model, which is part of an integrated flow, wave, transport and bed exchange model. The level of sophistication required for these sub-models or modules (and the accuracy and resolution of data required as inputs, forcing and for calibration) will depend on the purpose of the SPM module.

Remote sensing reflectance images are known to give excellent information on the seasonal variation of SPM, in particular its spatial patterns (Vos and Schuttelaar, 1995, 1997; Vos et al., 2000). These images are therefore well suited for calibration and validation of SPM models assessing reliability and predictive capability. In combining SPM models and observations, we must recognise the following.

(1) In principle, continuous SPM measurements are required because of the large natural (small-scale) variability of SPM concentrations (patchiness, tidal phase effects). Statistical methods may be used to retrieve both coherent means and associated small-scale variability from these measurements.

(2) Remote sensing observations in the North Sea require calibration and validation with in situ measurements (Vos et al., 2000). Extensive in situ data sets are available

from ZISCH (Sündermann, 1994) and from the NSP (Natural Environment Research Council, 1992). Large spatial coverage of the North Sea is obtained from remote sensing data, notably NOAA/AVHRR, for which high-quality processed data sets of weekly and monthly composite images exist.

(3) Knowledge of North Sea bed–sediment characteristics is varied. Information is found in the studies by Jarke (1956) and van Alphen (1987), from maps (for example, Figge, 1981; Geological Survey of The Netherlands, 1986; Balson et al., 1991; British Geological Survey (BGS)) and from the recent Holderness Coastal Experiment (Prandle et al., 2000). Since the source of sediment at the seabed may have a large natural variability, accurate quantification of erosion fluxes is not possible.

(4) The sophistication of SPM models is effectively limited by the amount of useful field data available to validate associated coefficients. Thus, the models here use only the simpler SPM concepts, usually having some four to six empirical parameters.

#### 4. 2D SPM model (rectangular coordinates)

This section aims to illustrate how best use can be made of the SPM observational data set obtained during the NSP (1988–1992) (see Lane et al., 2000). These data are used to indicate the source locations and a characteristic quantity (settling velocity) to allow meaningful simulations.

POL's (2D vertically averaged) General Purpose Model (Jones, 1999) was assembled specifically for the NSP. It is written in a modular form with the intention that it could be easily adapted to users' needs, to aid process studies. The NSP data are available on CD ROM (Natural Environment Research Council, 1992) and include vertical profiles of suspended sediment concentration collected at over a hundred fixed stations every month between August 1988 and October 1989. An example of the depth-averaged observed suspended sediment concentrations is shown in Fig. 2.

##### 4.1. Suspended sediment simulations — 35-km grid, tidally averaged

###### 4.1.1. Model concept

The 35-km depth-averaged version of the General Purpose Model is used to simulate the transport of suspended sediments in the North Sea. The model domain is limited to cover the southern North Sea from the Dover Strait to 55.5°N and includes the effects of advection, diffusion, settling of suspended sediments and resuspension. Sources of sediment are from the major rivers (Humber, Thames, Rhine, Elbe, Tyne/Tees), the Dover Strait and the northern boundary.

The model is based on the following advection–diffusion equation:

$$\frac{\partial C}{\partial t} + \underbrace{\left[ u \frac{\partial C}{\partial x} + v \frac{\partial C}{\partial y} \right]}_{\text{advection}} - \underbrace{\left[ E_x \frac{\partial^2 C}{\partial x^2} + E_y \frac{\partial^2 C}{\partial y^2} \right]}_{\text{diffusion}} = \underbrace{-\alpha C}_{\text{sink}} + \underbrace{\frac{k|\bar{u}|^n}{h}}_{\text{source}} \quad (1)$$

where  $C$  is the concentration of suspended sediment,  $t$  is time,  $u$  and  $v$  are residual current velocities in the east and north directions, respectively,  $h$  is the total water depth,

and  $\bar{u}$  is the tidal current amplitude.  $E_x$  and  $E_y$  are effective horizontal eddy diffusivities ( $\text{m}^2 \text{s}^{-1}$ ) in the east and north directions and include sub-grid scale advective effects. The sink and source terms are represented by simplified parameterisations of settling and resuspension. More sophisticated formulae are presented by van Rijn (1993).

The source term representing sediment resuspension at the seabed is set proportional to some power of  $\bar{u}$ ; corresponding incremental concentrations are then inversely proportional to the water depth. In the strongly tidal southern North Sea, we found that computed SPM concentrations are relatively insensitive to the power  $n$ , when  $n$  is 2, 3 or 4. We have used  $n = 3$ .

The settling of sediment is simulated using a simplified ‘half-life’ formula in which  $\alpha$ , the settling constant ( $\text{s}^{-1}$ ) is a function of  $w_s$ , the settling velocity of the suspended sediment and  $E_z$ , the vertical eddy diffusivity.

$$\alpha = 0.693 \frac{w_s^2}{E_z} \quad (2)$$

where  $E_z$  is the lesser of  $1/2 \beta \bar{u} h$  (shallow water) and  $\gamma \bar{u}^2$  (deep water),  $\beta$  is 0.0025, and  $\gamma$  is 0.2 s (see Prandle, 1998).

The advection in the model is forced by a linear combination of  $M_2$  tidal residual currents (computed by a hydrodynamic model version on the same schematisation), with wind-driven residual currents (wind stress of  $0.1 \text{ N m}^{-2}$ ) that are scaled by a seasonally varying wind field.

#### 4.1.2. Model simulations

Model runs are first completed for each of the above individual sources (Fig. 3). These are treated as a continuous specified concentration at the location of the source (e.g.  $10 \text{ mg l}^{-1}$ ). Settling velocities,  $w_s$ , used are:  $10^{-2} \text{ m s}^{-1}$  for sand,  $10^{-4} \text{ m s}^{-1}$  for silt and  $10^{-6} \text{ m s}^{-1}$  for clay. Model results for sand and silt fractions do not show much movement of material away from the coast since, for the model resolution and time steps used, most of the sediment has settled out of the water column. Simulations for clay do show movement of material from the coast, and the extent of this depends on the magnitude of the coefficient  $k$  in Eq. (1). The suspended sediment behaves as a passive tracer when the value of  $\alpha$  is sufficiently small.

The model time step is 1 day, and seasonal cyclic convergence occurs after 2 years of simulation, i.e. starting with zero concentrations, computed SPM concentrations in year 2 are the same for the equivalent stage of year 3, etc.

#### 4.1.3. Estimates of source terms

From multiple linear regression of the temporal variations in the spatial distributions from each individual source against the depth-averaged observed NSP suspended sediment concentrations, the magnitude of each source can be estimated and an indication of fractional contribution to the overall variance. This method has been used successfully by McManus and Prandle (1997). The initial regression analysis included

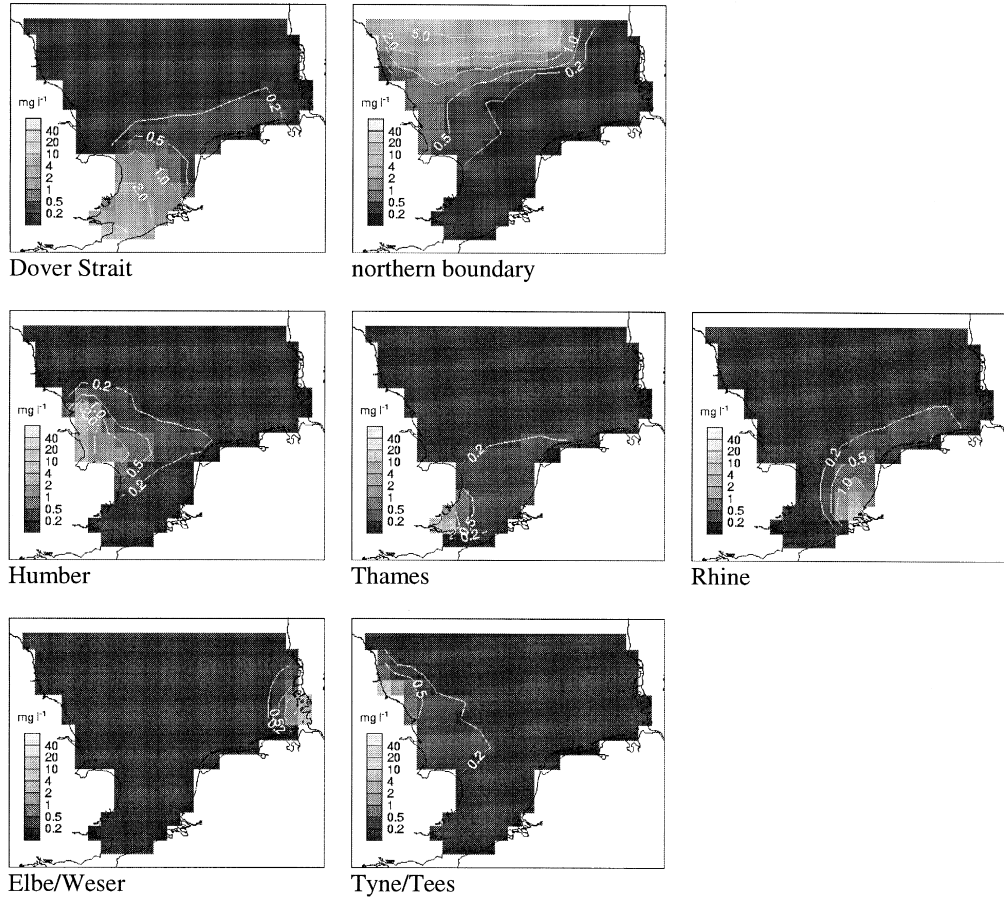


Fig. 3. Suspended sediment concentrations ( $\text{mg l}^{-1}$ ) in March, resulting from each source (with a constant concentration of  $10 \text{ mg l}^{-1}$  of clay, after 3 years).

Table 1

Regression coefficients and amplitudes for model sediment sources. The source amplitude is the scaling factor multiplied by the nominally assumed concentration of  $10 \text{ mg l}^{-1}$

	Fractional variance	Scaling factor
Humber	0.487	0.565
Thames	0.246	0.314
Elbe/Weser	-0.017	0.067
Tyne/Tees	0.085	0.097
Dover Strait	0.297	0.213

all sources; however, the source from the northern boundary was negligible, and the Rhine was assigned a negative regression factor. A subsequent analysis was completed without these two sources, giving a correlation coefficient of 0.61 and a mean sediment concentration of  $0.84 \text{ mg l}^{-1}$ . The results are given in Table 1, indicating that the largest sediment source concentrations in the southern North Sea are from the Humber, Thames and Dover Strait.

Riverine sediment sources into the North Sea are given by Pohlmann and Puls (1994), and are listed in Table 2 together with mean sediment concentrations (calculated by numerical model using these inputs — Section 4.2.3) close to these sources. The model values of suspended sediment concentrations near the Elbe estuary are much greater than suggested from Pohlmann and Puls; likewise, the model concentrations are much lower for the Tyne/Tees. However, from the other much larger sources, the concentrations agree to within a factor of four.

Table 2

Sediment sources at major rivers and model boundaries

	Mean river flow ( $\text{m}^3 \text{ s}^{-1}$ )	Sediment input ( $10^6 \text{ kg year}^{-1}$ ) <sup>a</sup>	Mean concentration from river source ( $\text{mg l}^{-1}$ )	Mean concentration calculated in nearest grid square ( $\text{mg l}^{-1}$ ) <sup>b</sup>
Humber/Holderness	189	50/500	8.3–83	34.4
Thames	67	240	113	25.5
Rhine	3139	750	7.5	29.5
Elbe/Weser	1770	768	13.7	83.2
Tyne/Tees	62	30	15.3	0.51
Dover Strait	$10^5$	13600	4.3	3.9
Northern boundary	–	–	–	< 0.5

<sup>a</sup>Values from Pohlmann and Puls (1994).

<sup>b</sup>Concentrations from 8-km grid model (Section 4.2.3).

#### 4.1.4. Determination of empirical parameters for settling velocities

In the absence of data on the distribution and type of sediment, a single sediment class is presently simulated in the model. Additionally, values for the empirical parameters  $k$ ,  $n$  and  $\alpha$  are currently specified. To determine values suitable for the spatial/temporal resolution of the model, the depth-averaged observations of suspended sediment concentrations were analysed. The residual currents from the hydrodynamic model, with suitable scaling to account for seasonal variation, were used to calculate the expected advection at each model grid-point. We assume the following conditions: (i) steady-state conditions prevail, i.e. is  $\partial C/\partial t = 0$ , (ii) for the model resolution of 35 km and time between quasi-synoptic suspended sediment observations of 1 month, advection dominates over diffusion. The settling constant  $\alpha$  can then be found from the relationship:

$$\alpha = \frac{1}{C} \left[ \frac{k|\bar{u}|^n}{h} - \text{advection} \right] \quad (3)$$

The settling constant is assumed to have a positive value, hence this sets a lower limit of  $k$  to be greater than  $k_{\min} = \text{advection} \times h/|\bar{u}|^n$ . The advection term in Eq. (1) is calculated by the numerical model, and  $k$  is then assigned the highest value of  $k_{\min}$  in the model domain.

We are now in a position to calculate values of settling constant in the model. The settling velocity can be calculated by combining Eqs. (2) and (3). Fig. 4 shows an example from the resulting seasonal spatial distributions of the settling velocity, and hence the likely sediment type. Coarser material ( $w_s > 0.01 \text{ m s}^{-1}$ , i.e. sand) occurs close to land and on offshore banks, and finer material ( $w_s < 5 \times 10^{-4} \text{ m s}^{-1}$ ) is found in deeper water.

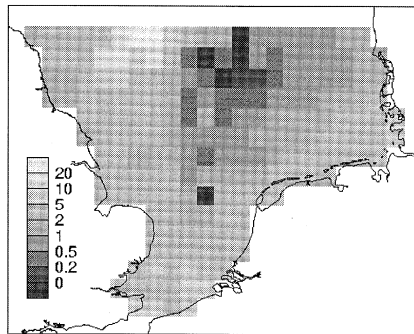


Fig. 4. Settling velocities ( $\text{mm s}^{-1}$ ) calculated from observed sediment concentrations and modelled advection for cruise CH47 (27/2–12/3/1989). Sand corresponds to the lighter grey regions, and clay corresponds to the darker grey regions.

#### 4.2. Suspended sediment simulations — 8-km grid, tidally resolving

##### 4.2.1. Model concept

The 35-km model grid spacing is too large to resolve the shallow coastal regions, and is also insufficient for sediment sources to be identified accurately. A higher resolution model was therefore required.

An 8-km version of the General Purpose Model was employed to carry out the suspended sediment simulation. The  $S_2$  tidal residual transports are included, in addition to  $M_2$  residuals and monthly varying wind-driven residuals. The model time-step is 15 min.

The sediment sources are again at rivers and the model open boundaries. This time, the model resolution is sufficiently fine so that the river sources can be specified as mass input rates (given in Table 2).

##### 4.2.2. Sedimentation and erosion

In addition to the source/sink terms from Eq. (1), simulations were also made using ‘threshold stress’ formulae (Eqs. (4) and (5)) to represent the deposition and erosion processes (from Odd and Murphy, 1992; Krone–Partheniades formulae).

$$dC_{\text{dep}} = \left[ 1 - \frac{\tau_b}{\tau_{\text{dep}}} \right] C_{\text{bed}} w_s \frac{dt}{h} \quad \text{for } \tau_b < \tau_{\text{dep}} \quad \text{otherwise } dC_{\text{dep}} = 0 \quad (4)$$

$$dC_{\text{ero}} = \left[ \frac{\tau_b}{\tau_{\text{ero}}} - 1 \right] E_0 \frac{dt}{h} \quad \text{for } \tau_b > \tau_{\text{ero}} \quad \text{otherwise } dC_{\text{ero}} = 0 \quad (5)$$

where  $C_{\text{bed}}$  is the suspended sediment concentration close to the seabed,  $\tau_b$  is the stress at the seabed. The threshold stress for deposition,  $\tau_{\text{dep}}$ , is assumed equal to that for erosion,  $\tau_{\text{ero}}$ , with a value of  $0.06 \text{ N m}^{-2}$ . The erosion rate  $E_0$  is  $0.1 \text{ kg m}^{-2} \text{ s}^{-1}$ . To simplify the calculations, we assume in this case that there is an unlimited supply of sediment at the seabed for resuspension and keep track of the amount of material in suspension as well as on the seabed.

##### 4.2.3. Model simulations

As in the 35-km model, cyclic convergence occurs after about 2 years. A 3-year simulation was completed using the mass inputs from Table 2 as the sediment sources. Simulations were carried out with the initial conditions of (i) zero suspended sediments, and (ii)  $10 \text{ mg l}^{-1}$  suspended sediment concentration. Both simulations converged to the same solution. The mean concentrations at the riverine source locations during the final year of the simulation are listed in Table 2 (see Fig. 5, and compare with Fig. 1). For the Tyne/Teas, Thames and Dover Strait, the model concentrations are smaller than the riverine source — indicating rapid dilution. Conversely, for the Humber, Rhine and Elbe, the offshore concentration is greater than the riverine source — indicating localised retention with subsequent cycles of deposition and resuspension.

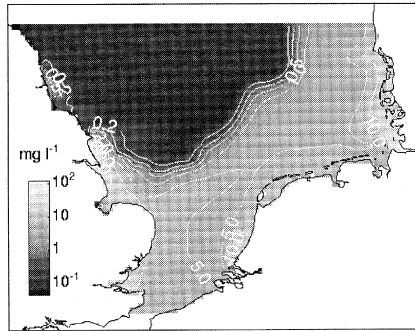


Fig. 5. Depth-averaged suspended sediment concentrations predicted by the 8-km grid model in March of year 3, resulting from the (clay) sources given in Table 2.

Direct comparison with observations is complicated by (i) availability and poor time/space resolution of direct observations, (ii) sharp gradients of suspended sediment concentrations close to the sources. It is therefore more realistic to compare, instead, patterns in the model results with that of observations rather than the absolute values (see for example, the curvilinear approach in Section 5).

### 5. 3D and 2D SPM model (curvilinear grid)

In this section, a sensitivity analysis of the modelling of North Sea SPM distribution and its seasonal distribution is presented. A curvilinear grid in 2D and 3D is used together with NOAA satellite reflectances in the assessment (Boon et al., 1997; Gerritsen et al., 2000). We first discuss the specific model set-up and key model aspects such as the net hydrodynamic volume transport, the inclusion of wind-wave effects in the SPM model, the formulation of settling, erosion and sedimentation processes in 2D and 3D, and the effect of stratification. In subsequent subsections, the sensitivity analysis for the 2D model application and the 3D model application (on the same grid) are discussed.

It is noted once again that the aim in the modelling simulation is to reproduce the North Sea scale SPM patterns and their seasonal variations — not individual localised, short-lived events. With its synoptic nature, remote sensing image data are more suited for validation than much of the in situ data. The focus is on using NOAA/AVHRR images for SPM, while using a structured modelling approach to assess results and sensitivities (see also Vos et al., 2000).

Modelling SPM correctly on a seasonal scale requires a chain of models or modules forming an integrated model. This sequence is outlined below.

- A hydrodynamic model for tidally and meteorologically induced flows, with inclusion of salinity variation and a model for the turbulence parameters. The model domain, model grid and related gridded model geometry and bathymetry should be

designed to reflect the requirements of the SPM transports, rather than the hydrodynamics per se.

- A wave module to generate wave characteristics that are key parameters in bed erosion. Here, the wave-induced bed shear stress is the relevant parameter rather than accurate wave spectra.

- The SPM transport model based on the hydrodynamic database, to which is linked a module describing the sedimentation and erosion processes and flocculation of silt.

There are uncertainties associated with each module and the resulting errors propagate from one module to the next (see Fig. 1 of Vos et al., 2000). To make an assessment of the SPM modelling, we need to qualitatively analyse the uncertainties due to: specification of bathymetry, hydrodynamics (effect on residual flow), meteorological forcing (fixed wind or spatially and temporally varying wind), wind–waves and stratification and inputs such as dumping and coastal erosion.

The uncertainties due to parameter variations of the SPM model are quantified and ranked employing a ‘Goodness-of-Fit’ (GoF) concept outlined by Vos et al. (2000) or, in more detail by ten Brummelhuis et al. (2000).

### 5.1. Model set-up and hydrodynamics

The model area and model grid were selected by taking into account the objectives of this modelling, i.e. accurate simulation of the large-scale spatial behaviour of suspended matter in the region. Given the importance of sediment fluxes through the Dover Strait, the model domain was extended into the English Channel. The grid was designed to reflect the requirements of all processes in the integrated model, which led to the following grid characteristics: (1) an orthogonal curvilinear boundary fitted grid design that is sufficiently detailed and smooth in the Dover Strait to represent the local flows and sediment transport; (2) a grid design that allows for a proper numerical representation of the strong cross-shore SPM gradients in the near-coastal zone. Attention has been given to the interfacing with an encompassing model in view of meteorological forcing, in order to analyse the sensitivity to propagation of uncertainties and errors in such linking; (3) highest resolution in the near-coastal zone where most of the sediment transport and processes take place; and (4) a  $\sigma$ -coordinate approach (for the 3D simulations) to ensure sufficient vertical resolution in the near-coastal zone.

In view of computational flexibility, the number of horizontal computational elements is limited in the central parts of the model area. The resulting model grid is shown in Fig. 6.

The hydrodynamic basis of the suspended matter modelling is created by applying the hydrostatic inhomogeneous tide resolving 2D and 3D shallow water equations including a  $k$ - $\varepsilon$  turbulence model on a general orthogonal curvilinear grid (Delft3D, 1997). The gridded bathymetry with varying detail was constructed merging available model bathymetries of North Sea Model Advection Dispersion Study (NOMADS) and PROMISE partners. The bathymetry and open boundary tidal forcing (obtained by nesting the model in the shelf-wide model Dutch Continental Shelf Model (DCSM) were adjusted by applying adjoint modelling techniques and water level criteria, using the model in 2D mode (ten Brummelhuis et al., 1997). In the historic hindcast simulations

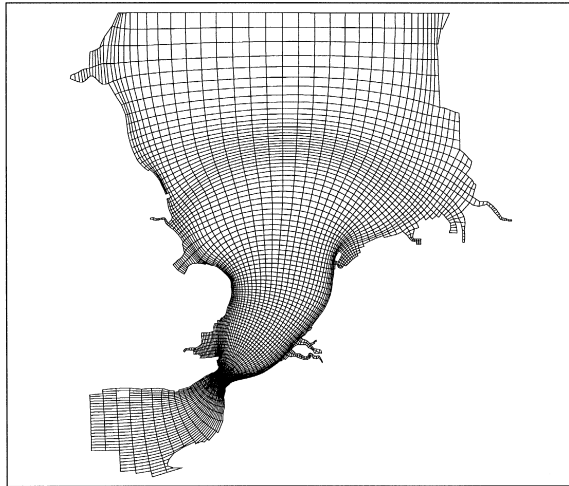


Fig. 6. The curvilinear computational model grid (3915 elements).

for the year 1994, space- and time-varying historic meteorological forcing were prescribed (courtesy of the Norwegian Meteorological Institute). Yearly averaged fresh water river outflows were prescribed and the model was ‘spun up’ for 12 months to initialise the horizontal salinity distribution and the bed surface sediment distribution. The model time step was 5 min.

The 3D model simulation was directly derived from the 2D model set-up defining 10  $\sigma$ -layers. Turbulence was modelled by a  $k$ - $\varepsilon$  model (Uittenbogaard and van Kester, 1996; Uittenbogaard et al., 1992, 1996). Salinity was modelled in 3D since salinity stratification occurs in coastal zones (river Rhine outflow). Temperature was not modelled since it mainly affects stratification in the northern North Sea (Uittenbogaard and van Kester, 1996), where SPM concentrations are low ( $< 2 \text{ mg l}^{-1}$ ). Wave–current interaction and wave-induced flow are not considered.

### 5.1.1. Residual flow

*5.1.1.1. Residual volume fluxes and transit times.* In SPM transport models, the (residual) flow field is effectively an input or forcing, and uncertainties in the prescribed flow may have a large influence on the SPM transport results. Residual volume fluxes and related transit times have been studied intensively by various authors. Most studies combine information from tracers released from nuclear power plants at Cap de la Hague and Sellafield with transport models (see e.g. Prandle, 1984; Salomon et al., 1995). Recently, different monitoring techniques such as HF (high frequency) Radar and the Acoustic Doppler Current Profiler (ADCP) have been applied (Prandle et al., 1996). Table 3 presents information from the literature on modelled and measured residual volume fluxes through the Dover Strait for various situations, with tide and for tide plus

Table 3

(Modelled) long-term net volume fluxes through Dover Strait ( $\times 10^3 \text{ m}^3 \text{ s}^{-1}$ )

Source	Tide only	Tide + average wind	Remarks
Prandle, 1978	115	155	$M_2$ tide; southwest wind
Prandle, 1984	50	90	Based on $^{137}\text{Cs}$ tracer data;
Salomon and Breton, 1993	37	149	$\tau_{\text{wind}} = 0.07 \text{ Pa}$ (southwest direction) Averaged wind is southwest $8 \text{ m s}^{-1}$ ;
Salomon et al., 1993	38	114	$\tau_{\text{wind}} = 0.13 \text{ Pa}$ Averaged wind over period 1983–1991
Prandle et al., 1996	36	94	Based on HF Radar and ADCP field data

time- and space-averaged winds. The simulations show that the volume flux through the Dover Strait for a spring tide is twice that of the mean tide (calm wind conditions; Salomon et al., 1995). Wind speed and especially wind direction also have a large impact on the residual volume flux. Modelled monthly averages of residual volume fluxes for 1989 (Salomon and Breton, 1993) may vary by a factor five:  $57\,000 \text{ m}^3 \text{ s}^{-1}$  (June, calm winds) and  $289\,000 \text{ m}^3 \text{ s}^{-1}$  (December, strong winds). The yearly averaged residual volume flux was found to be  $114\,000 \text{ m}^3 \text{ s}^{-1}$ . Clearly, available estimates of residual volume fluxes and transit times contain many uncertainties partly due to the definition applied, which is directly reflected in the modelled behaviour of SPM transport.

*5.1.1.2. Net volume fluxes from the present curvilinear model.* The characterisation of sensitivities listed below is the result of extensive variations in gridded bathymetry, wind forcing, and grid design (fixed grid spherical versus curvilinear) in tide resolving simulations for the period March–September 1994 (Boon et al., 1997).

- For tide and fixed (persistent) averaged wind simulations, the mean residual volume flux agrees with the order of magnitude reported in the literature. Bathymetry and grid variations (rectangular versus curvilinear) had limited influence, with values  $73\text{--}107 \times 10^3 \text{ m}^3 \text{ s}^{-1}$ .

- For tide-only simulations, bathymetry variations have a much stronger influence, as has the use of the boundary-aligned grid, which leads to a strongly reduced tidal residual volume flux compared to modelling using a rectangular (coarse) grid approach ( $\sim 8 \times 10^3 \text{ m}^3 \text{ s}^{-1}$ ).

- For tide and historic time- and space-varying wind forcing, the instantaneous response of the volume flux to wind variations is strong, while the net residuals for months with low or not persistent wind effects are much lower than literature values.

- For months with a persistent meteorological forcing, the net residual volume fluxes more or less agree with values from literature.

- Persistent southwest winds during March 1994 accounted for 60% of the net residual volume flux during this 7-month period.

The main conclusion from this model sensitivity analysis is that the response of (residual) volume fluxes to fluctuating meteorology is likely to be a large source of

error. This suggests the need for a fundamental improvement of the air–sea momentum exchange concept for long-term flow modelling. Until then, the present common approach of calibrating long-term volume fluxes using time-averaged (persistent) wind estimates (Salomon et al., 1995) is best practice.

*5.1.1.3. Transit times of radionuclides discharged at Cap de la Hague.* An estimated mean persistent wind of  $7 \text{ m s}^{-1}$  from the southwest was used in a 2D model to determine transit times of a tracer patch released from Cap de la Hague (1st March 1994). This was compared with 2D model-based long-term transit time results calibrated on experimental radionuclide data from Salomon et al. (1995). The results are shown in Fig. 7 and compare well. The model results also compare well with residual volume flux estimates from HF Radar and ADCP by Prandle et al. (1996), but deviate from these for high winds and very calm conditions.

### 5.1.2. Wind-induced waves

We include wave effects-only in the modelling of erosion and resuspension of SPM as a first approximation. The magnitudes of the bed shear stress due to flow and the tide-averaged effect of wind–waves are assumed to be additive:

$$\tau = \tau_{\text{waves}} + \tau_{\text{flow}} \quad (6)$$

A detailed wave model for the whole North Sea, to link with the present SPM model, would be too demanding. The approach followed determines the values of  $\tau_{\text{waves}}$  using hindcast wave parameters from the coarser grid WASA model results for the North Sea (WASA Group, 1995). These are transferred as estimates for the coastal areas modelled with greater detail in the curvilinear grid, taking into account wind and wave direction, fetch length, shielding, and varying depth toward the coast (see van Vledder, 1997; Monbaliu et al., 1999).

Bed stresses increase markedly from the open North Sea towards the coast. The transformation of these WASA gridded wave parameters takes into account the changing depths and varying wind and wave directions, to determine suitable wave parameters on the detailed curvilinear grid in the near coastal zone. It is applied to each model grid point and for each time step that WASA wind and wave information is available (i.e. 3 h).

Fig. 8, for example, quantifies the effect of wind waves in terms of the suspended matter concentrations, by showing the relative difference of the SPM distribution for simulations with and without wave effects in the bed stress (2D model set-up). When interpreting this figure, the surficial bed sediment should be taken into account. Although wave stirring increased the bed stress in the Thames Estuary and at the Flemish Banks at that specific moment, no increase in the concentration occurred due to the lack of further erodible surficial sediments in the model. For the Flemish Banks, results do not agree with the data of Jarke (1956) and van Alphen (1987, 1990), indicating the presence of silt. The SPM concentrations in the Wadden Sea area can be as much as twice that in the German Bight, indicating that locally, additional bed material is available for erosion. Balanced descriptions of both the bed stress and the

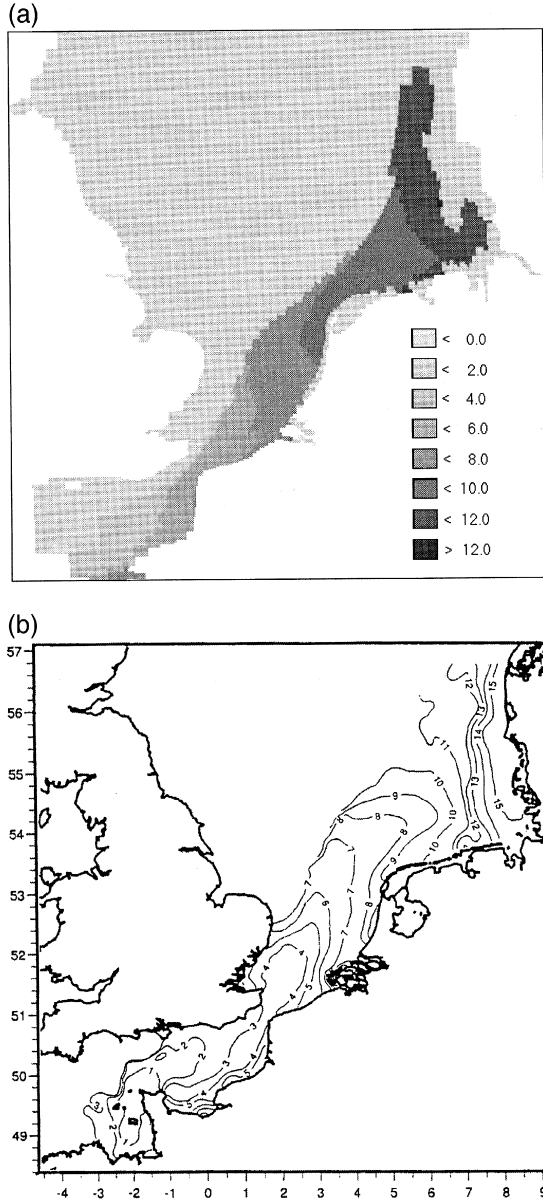


Fig. 7. (a) Modelled transit times in months; present curvilinear 2D model, fixed southwest wind  $7.5 \text{ m s}^{-1}$ , simulation over 12 months. (b) Modelled transit time (months) from Cap de la Hague for technetium, averaged over the period 1983–1992 (after Solomon et al., 1995).

available surficial sediment amount are important for SPM modelling (see next subsection).

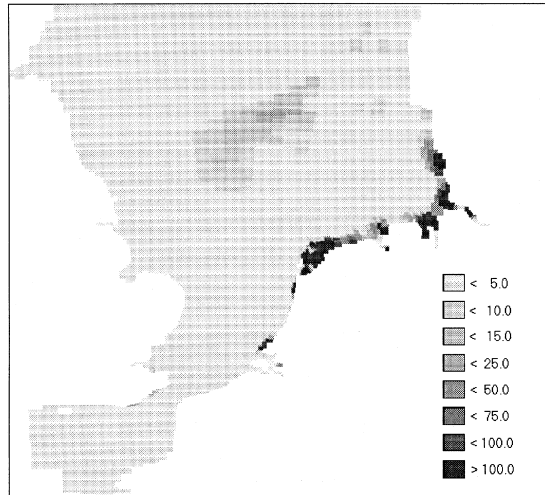


Fig. 8. Relative difference of 2D modelled SPM concentrations with and without wave effects included in the bed stress:  $100 \times (C_{\tau_{\text{flow} + \text{waves}}} - C_{\tau_{\text{flow}}}) / C_{\tau_{\text{flow} + \text{waves}}}$ , 00:00 GMT 30th April 1994.

5.1.3. Sedimentation and erosion processes

For the transport of substances in 2D and 3D including erosion–sedimentation processes, matching advection–dispersion modules were used, which include a range of process formulations (Delft3D, 1997). The model dynamically simulates the transport and fate of suspended matter in the water column and the top layer of the bed sediment. Sedimentation and erosion processes are based on the Partheniades–Krone concept (Krone 1962; Partheniades, 1962).

5.1.3.1. Sedimentation. A characteristic feature of cohesive sediments is the ability to form aggregates (flocs) that settle to the bed. Whether or not a particle will settle to the bed depends upon its size, density and the chemical conditions of the surrounding water system. Sedimentation is the process describing the settling of particles within the water column. This sedimentation process is described with the formulation by Krone (1962). The rate of downward mass transport (sedimentation) is equal to the product of the near-bed settling velocity, the near-bed concentration and a threshold factor. The sedimentation or deposition (Krone, 1962) is given by:

$$f_{\text{sed}} = P_{\text{sed}} w_s C_{\text{bed}}$$

$$\text{limitation: } f_{\text{sed}} = \min \left[ f_{\text{sed}}, \frac{C_{\text{bed}} h}{\Delta t} \right]$$

$$P_{\text{sed}} = \max \left[ 0, 1 - \frac{\tau}{\tau_{c,\text{sed}}} \right] \tag{7}$$

where  $f_{\text{sed}}$  is the sedimentation flux of SPM ( $\text{kg m}^{-2} \text{s}^{-1}$ ),  $\Delta t$  the model time step (s),  $h$  the average water depth (m),  $w_s$  the settling velocity of SPM ( $\text{m s}^{-1}$ ),  $C_{\text{bed}}$  the concentration of SPM near the bed ( $\text{kg m}^{-3}$ ),  $P_{\text{sed}}$  the sedimentation factor,  $\tau$  the bed shear stress (Pa) and  $\tau_{c,\text{sed}}$  the critical shear stress for sedimentation (Pa). Eqs. (4) and (7) differ in that the latter formally assumes an upper limit to the sedimentation rate to avoid negative concentrations in the model.

*5.1.3.2. Settling velocity  $w_s$ , 2D model.* Various laboratory and field measurements show that the suspended matter concentration strongly influences the aggregation process and thereby the settling velocities of the aggregates. Large-size flocs are denser and have higher settling velocities. In 2D, the effect of the sediment concentration on the flocculation process can be described by the following common formula (after van Leussen, 1994):

$$w_s = \lambda C^m \quad (8)$$

where  $w_s$  is the settling velocity ( $\text{m s}^{-1}$ ),  $\lambda$  the velocity conversion constant ( $\text{kg}^{-m} \text{m}^{3m+1} \text{s}^{-1}$ ), and  $C$  the suspended matter concentration ( $\text{kg m}^{-3}$ ).

The settling velocity is not constant in time and space for values of  $m \neq 0$  used. In the literature,  $m$  ranges from 0 to 2 (van Leussen, 1994). The spread in settling velocities increases with  $m$ . Therefore, for larger  $m$ , more size fractions of sediment are effectively lumped into the single fraction model. In coastal areas where concentrations and concentration gradients are high, large spatial differences in settling velocities are obtained with this approach. This mimics the presence of various fractions in these areas.

*5.1.3.3. Erosion.* Erosion of seabed material occurs when the bed shear forces exceed the resistance of the bed sediment. The resistance of the bed is characterised by a certain critical erosive shear stress. This critical stress is determined by several factors, such as, the chemical composition of the bed material, particle size distribution and bioturbation. Since often only qualitative information on the type of bed is available, usually a uniform value for this critical shear stress is employed in large-scale models. Erosion of sediment is induced by the bed stress due to tidal and wind-induced advective flows and surface waves.

Erosion is directly proportional to the excess of the applied shear stress over the critical bed shear stress for erosion. The erosion of homogeneous beds is based on the resuspension formula of Partheniades (1962):

$$f_{\text{res}} = P_{\text{res}} E_0$$

limitations: (1)  $f_{\text{res}} = 0$  if  $h < h_{\text{min}}$

$$(2) f_{\text{res}} = \min \left[ f_{\text{res}}, \frac{DM}{\Delta t A} \right]$$

$$P_{\text{res}} = \max \left[ 0, \frac{\tau}{\tau_{c,\text{ero}}} - 1 \right] \quad (9)$$

Table 4  
Sedimentation characteristics

Parameter	Value	Reference
Critical stress for sedimentation ( $\tau_{c, \text{sed}}$ )	0.04 Pa	Nicholson and O'Connor, 1986
	0.05–0.25 Pa	Winterwerp, 1989
	0.10–0.12 Pa	Amos and Mosher, 1985
Settling velocity ( $w_s$ )	0.27–2.1 mm s <sup>-1</sup>	Amos and Mosher, 1985
	0.01–0.1 mm s <sup>-1</sup>	Mehta, 1986
Settling velocity constant $\lambda$	0.513	Thorn, 1981 (Severn Estuary)
Settling velocity constant $m$	1.33	Krone, 1962 (San Francisco Bay)
	1.29	Thorn, 1981 (Severn Estuary)
$(w_s = \lambda C^m)$	1.2	van Leussen, 1994 (Ems Estuary)
	1.37	Burt, 1986 (Thames Estuary)
	1.04	Puls et al., 1988 (Elbe Estuary)

where  $f_{\text{res}}$  is the erosion rate (kg<sub>DW</sub> m<sup>-2</sup> s<sup>-1</sup>),  $P_{\text{res}}$  the erosion threshold factor,  $E_0$  the first-order erosion rate (kg<sub>DW</sub> m<sup>-2</sup> s<sup>-1</sup>),  $\tau$  the bed shear stress (Pa),  $\tau_{c, \text{ero}}$  the critical shear stress for erosion (Pa),  $h_{\text{min}}$  the minimal water depth for erosion (default 0.1 m) and DM/A the amount of locally available dry matter, expressed as dry weight per unit square (kg<sub>DW</sub> m<sup>-2</sup>). Eqs. (5) and (9) differ in that in the latter, the limitation by the available erodible surface sediments is formally included.

The value of  $E_0$  strongly depends on the sediment properties and environmental parameters. In this model, the erosion rate is limited by the available amount of sediment, which has settled in previous periods.

A first estimate of suitable parameter values for North Sea sedimentation and erosion of suspended matter is obtained from laboratory and field experiments quoted in literature. Tables 4 and 5 summarise some typical ranges of sedimentation and erosion parameter values found for estuaries and coastal zones.

The wide ranges found, sometimes factors of 10 or more, show that model parameters serve as bulk parameters in which different detailed processes are lumped. As argued above and in more detail in Vos et al. (2000), given the level of information in the data, we consider it unwarranted to model these processes with much more detail.

*5.1.3.4. Settling velocity in 3D modelling.* In 2D modelling, the water column is assumed to be always completely mixed, so the settling velocity  $w_s$  is vertically

Table 5  
Erosion characteristics

Parameter	Value	Reference
Critical stress for erosion ( $\tau_{c, \text{ero}}$ )	0.05–0.4 Pa	Mehta et al., 1982
	0.1–0.5 Pa	Winterwerp, 1989
Erosion rate $E_0$	0.01–0.5 g m <sup>-2</sup> s	Winterwerp, 1989
	0.002–0.02 g m <sup>-2</sup> s	Kappe et al., 1989

uniform. In 3D modelling, the vertically varying settling velocity  $w_s$  in combination with the vertical diffusion coefficient given by the hydrodynamic  $k$ - $\varepsilon$  module, determines the sedimentation flux. Information from the literature on suitable  $w_s$  values for regional scales like the North Sea is limited, and most experimental information refers to settling velocities for estuaries and coastal zones. The effect of vertical variation may be illustrated on the analytic solution in one-dimensional vertical (1DV) of the stationary transport problem with vertical diffusion and concentration-dependent settling velocity and no net sedimentation or erosion.

$$C(z) = \left[ \frac{\lambda m z}{D} + C_{\text{bed}}^{-m} \right]^{-1/m} \quad (10)$$

where  $z$  is the distance from the bed (m),  $C_{\text{bed}}$  the SPM concentration at the bed ( $z = 0$ ) ( $\text{kg m}^{-3}$ ),  $D$  the vertical diffusion coefficient ( $\text{m}^2 \text{s}^{-1}$ ),  $m$  the power of concentration-dependent settling ( $m > 0$ ), and  $\lambda$  the velocity conversion constant ( $0.001 \text{ kg}^{-m} \text{ m}^{3m+1} \text{ s}^{-1}$ ).

This equation shows the basic concept for 3D: a steep decrease in concentration from the water surface to the seabed for finite vertical diffusivity with  $D < 0.001 \text{ m}^2 \text{ s}^{-1}$  for the values of  $\lambda = 5.13 \times 10^{-4} \text{ kg}^{-m} \text{ m}^{3m+1} \text{ s}^{-1}$  and  $m = 1.29$  that were used. For the 2D case, one must substitute an infinite value for  $D$  ( $D = 1.0 \times 10^{-2} \text{ m}^2 \text{ s}^{-1}$  readily suffices), and a well-mixed column results. In 3D, the settling velocity (as a function of  $\lambda$  and  $m$ ) clearly has an effect for small diffusion, e.g. with stratification and concentration differences within the water column. Analogous to the 2D case, the settling velocity near the bed will determine the sedimentation flux.

#### 5.1.4. Stratification and turbulence

Stratification may have an important effect on the vertical distribution of cohesive sediment in the water column. Before embarking upon large-scale 2D and 3D simulations, a computationally simple but conceptually rather refined 1DV model was applied to study the importance of temperature and salinity for the distribution of sediment over the water column. This 1DV model, or ‘point model’ describes the transport of momentum, temperature, turbulent kinetic energy ( $k$ ) and the dissipation rate of turbulent kinetic energy ( $\varepsilon$ ) in a vertical water column with high resolution, accommodating various sediment fractions (Uittenbogaard and van Kester, 1996; Uittenbogaard et al., 1996).

As our interest is in the exchange of the coastal zone, i.e. shallow water and high silt concentrations and gradients, with the open water, we consider ( $H < 35 \text{ m}$ ,  $Bh/U^3 < 2$ ). Here,  $U$  and  $B$  are the maximum velocity and buoyancy flux, respectively, and  $Bh/U^3$  is the dimensionless Simpson–Hunter parameter to determine the potential for stratification (Simpson and Hunter, 1974). For deeper water and  $Bh/U^3 > 3$ , i.e. temperature stratification may occur, silt concentrations are low ( $< 2 \text{ mg l}^{-1}$ ).

For homogeneous salinity distributions and realistic sea surface temperatures in the North Sea,  $Bh/U^3 \sim 2.0$  and depths of  $H = 20$  and  $H = 35 \text{ m}$ , the 1DV calculations showed that the effect of temperature on sedimentation is negligible. For the vertical inhomogeneous salinity case, the simulations showed that the effect of salinity on

settling velocity and sedimentation can be significant, so salinity stratification should be included. A combined effect on stratification of both salinity and temperature was not considered.

## 5.2. Results of the SPM transport model in 2D and 3D, ranking of sensitivities

### 5.2.1. Objective, GoF

The objective of the modelling and the simulations is the representation of the North Sea SPM patterns and their variation over the seasons. Generally, the coverage of the SPM in situ data is relatively sparse in the North Sea, is rarely synoptic and shows a high natural temporal variability. NOAA/AVHRR reflectance images give a synoptic view and can be processed into consistent regional-scale SPM patterns (see Section 3). We have therefore chosen (surface) concentrations based on NOAA reflectance data of 1994 as data against which we compare the modelled representation of the seasonal SPM patterns. The NOAA images used are processed monthly composites and therefore ideally suited to give information on the variation in SPM patterns over periods of months (images provided courtesy of the Royal Netherlands Meteorological Institute).

For an objective, quantitative and reproducible comparison of model data represented on varying grid box sizes with concentrations derived from monthly composite NOAA reflectance images, the GoF concept introduced in Vos et al. (2000) was applied. The essence of this method is based on a subdivision of the model area into characteristic zones, such that the variation of the NOAA reflectance intensity over a given zone is limited. Fifteen characteristic zones were defined. Averaging of a given NOAA image-based concentration field per zone leads to a limited set of zonally averaged concentrations. Applying the same to the corresponding monthly averaged modelled concentrations, a least squares criterion or GoF for the level of agreement between model results and data is defined using only these  $2 \times 15$  aggregated values. For details, one is referred to Vos et al. (2000).

The 2D simulations covered the period March–September 1994 (7 months). This corresponds to starting with a winter situation with strong winds and erosion effects, and ending with a fully developed summer situation. For the 3D simulations, the period April–July (4 months) was considered, which enables a comparison with the 2D simulations for the period April–July. We note that in 3D, the modelled surface concentrations are used in the GoF, while in the 2D model, the modelled depth mean concentrations are used, representing a first approximation for the behaviour at the surface. The simulations in this subsection complete the (more qualitative) considerations of the sensitivities to both variations in model forcing and options in process description given in the previous subsection.

### 5.2.2. Sensitivity analysis in 2D

Based on the considerations and schematic comparisons described in the previous section, we assume the following empirical parameters with their initial values for the 2D case: (1) settling velocity  $w_s = \lambda C^m$ , with  $\lambda = 5.13 \times 10^{-4} \text{ kg}^{-m} \text{ m}^{3m+1} \text{ s}^{-1}$  and  $m = 1.29$  (Thorn, 1981); (2) erosion rate  $E_0 = 0.2 \text{ g m}^{-2} \text{ s}^{-1}$  (Boon and Baart, 1996); (3) critical shear stress for sedimentation  $\tau_{c, \text{sed}} = 0.10 \text{ Pa}$ ; (4) critical shear stresses for

erosion  $\tau_{c,ero} = 0.75$  Pa, based on comparing Boon and Baart (1996) and van Alphen (1987); (5) scale factors ‘ $D_i$ ’, for uncertainties in dumping data, and accounting for return of part of the dumped sediment to the dredging location, and not entering the North Sea system (retention factors):  $D_H$  (Humber),  $D_L$  (Loswal Noord) and  $D_Z$  (Zeebrugge and Oostende), see Table A1; (6) scale factors ‘ $S_i$ ’, for the amounts of coastal erosion (e.g. Holderness  $S_H$ , Norfolk  $S_N$ , and Suffolk  $S_S$ ). Initial settings of these numbers were taken from Odd and Murphy (1992), see Table A1; and (7) scale factors ‘ $B_S$ ’ for the concentration of SPM prescribed at the southern open model boundary (transect Cherbourg–Southampton, initial SPM distribution in time taken from Boxall et al. (1995); uniformly applied along the boundary). At the Atlantic open boundary, the SPM concentration was assumed to be constant at  $2 \text{ mg l}^{-1}$ .

This results in a total of 12 uncertain parameters that were varied in the sensitivity analysis of the SPM model:  $\lambda$ ,  $m$ ,  $\tau_{c, sed}$ ,  $\tau_{c, ero}$ ,  $E_0$ ,  $D_H$ ,  $D_L$ ,  $D_Z$ ,  $S_H$ ,  $S_N$ ,  $S_S$  and  $B_S$ . All were assumed constant in time and independent of spatial coordinates.

A series of simulations with single parameter variations were made. The initial values of the parameters  $\tau_{c, sed}$ ,  $\tau_{c, ero}$ ,  $E_0$ ,  $S_H$ ,  $S_N$ ,  $S_S$ ,  $D_Z$ ,  $B_S$  were simply halved and doubled whereas for the others, more specific changes were investigated. A final simulation was made in which an intra-annual time variation was applied to the annual coastal erosion inputs based on the time history of the area-averaged wind stress.

Results of 23 model sensitivity simulations in terms of the percentage change of the GoF with respect to a run with the above initial parameter settings (run 0) are shown graphically in Fig. 9.

The largest relative difference results from a doubling of the input due to coastal erosion at Holderness (case 10). The largest model improvement follows for doubling  $\tau_{c, ero}$  (case 4), leading to a value  $\tau_{c, ero} = 1.5$  Pa. This parameter value is rather high and

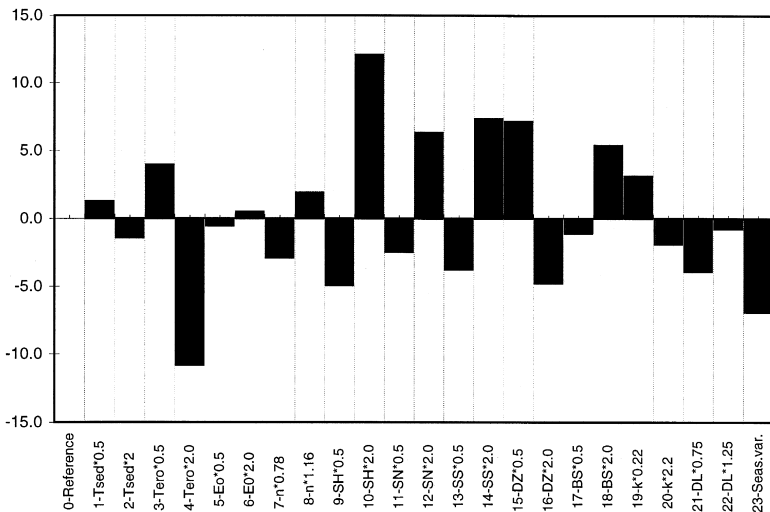


Fig. 9. Change of the GoF criterion in percentage for 23 sensitivity simulations with the 2D SPM model, relative to a reference simulation (index 0). Simulation period 1st March–1st October 1994.

suggests that erosion occurs only at high wind speed, and/or in areas with much wave activity. Increasing  $\lambda$  (settling velocity) by more than a factor of two gives rise to only a small effect (case 20). Cases 9, 11 and 13, representing the effect of halving the assumed input due to coastal erosion at Holderness, Suffolk and Norfolk, indicate that the inputs should be less than those given in Odd and Murphy (1992) and perhaps more in line with McCave (1987) and McManus and Prandle (1997). There is no good explanation yet why these results predict an increase of the dumping at Zeebrugge and Oostende (case 16; doubling of the reference value). The results of case 23 confirm the model assumption that erosion is not uniformly distributed over the year, and is correlated to wind stress.

A further aspect is the present assumption of constant and spatial uniform parameters, which, e.g. for sedimentation and erosion parameters, will be too simple. More detailed experimental information is required on the ranges of the various processes and parameters, including data on surficial bed sediments available for erosion. Improved parameter formulations should be derived from such information.

The results highlight the complexities of suspended matter modelling. Fig. 9 shows six single parameter variations (cases 4, 9, 13, 16, 21 and 23) that lead to a reduction of more than 4% in the GoF criterion. Only one of these exceeds a 10% reduction (case 4). The present model variations are clearly insufficient for optimising the model in terms of adjusting the parameters to give a minimum value for the GoF criterion. Combined variations will need to be assessed, e.g. as outlined by the section on adjoint modelling (see ten Brummelhuis et al., 2000; Vos et al., 2000).

### 5.2.3. Sensitivity analysis in 3D

The 3D sensitivity analysis focussed on the one concept that is essentially different from 2D, namely the settling velocity  $w_s$ . Section 5.1.3 presented some concentration-dependent 2D formulations applied in estuaries. For 3D and regional scales, a dependence on concentration is unclear from the outset. The conceptual relation  $w_s = \lambda C^m$  was retained, with  $\lambda$  having dimension [ $\text{kg}^{-m} \text{m}^{3m+1} \text{day}^{-1}$ ]. Five simulations were made, varying  $w_s$ , and results were compared with the 2D results, all for the period April–July 1994. The remaining basic model parameters are unchanged from the 2D case, apart from the bed stress assumption  $\tau_{\text{wave}} = 0$ , which however is expected to have limited influence for the period of simulation. Table 6 defines the five 3D cases considered.

The first three simulations differ in the definition of  $w_s$ . We assume a seasonal dependence of all coastal erosion inputs in simulations 4 and 5: the annual average at April, half this value in July and an overall reduction to 72% for these 4 months. This is because of the large influence of coastal erosion in 2D and the conclusions relating to the uncertainties in coastal inputs from the adjoint analysis in Vos et al. (2000), and is based on the seasonal distribution applied in simulation 23 of the previous subsection. In these simulations, parameter settings ( $\lambda = 5$ ,  $m = 0$ ) and ( $\lambda = 0.5$ ,  $m = 1$ ) were assumed, respectively. Fig. 10 presents the results, using remote sensing data and surface layer model results in the GoF.

These results show that: (1) the reference simulation with a constant settling velocity of  $5 \text{ m day}^{-1}$  compares very well with the 2D model result (a difference of 8% is

Table 6  
Definition of 3D sensitivity simulations

Simulation number	Coefficient $\lambda$ ( $\text{m day}^{-1} \text{ m}^{3m} \text{ kg}^{-m}$ )	Power $m$	$w_s$ ( $\text{m day}^{-1}$ )	Remarks
0	44.3232	1.29	$w_s = \lambda C^m$	2D case
1	5	0	5	Reference simulation
2	10	0	10	Doubled $w_s$
3	0.5	1	$w_s = \lambda C^m$	Concentration dependence
4	5	0	5	Reduced coastal erosion
5	0.5	1	$w_s = \lambda C^m$	Reduced coastal erosion

found); (2) the simulations with doubled and concentration-dependent settling velocity — ( $\lambda = 10, m = 0$ ) and ( $\lambda = 0.5, m = 1$ ) — drastically improve results (GoF reductions of 22% and 50%), that is, the SPM patterns of the upper model layer agree much better with the NOAA data patterns. The fall or settling velocity should clearly be concentration-dependent, with linear dependence a good first approximation. The spatial distribution of the settling velocity  $w_s$  of the top layer for 5th July 1994 for simulation 3 is plotted in Fig. 11, which shows that in the Dutch coastal zone,  $w_s$  is of the order of 10–30  $\text{m day}^{-1}$ ; (3) the significance of a concentration-dependent settling velocity is easily shown for the coastal zone, when the water column becomes stratified. Fig. 12 presents the daily averaged time histories of SPM for Hoek van Holland for the model top layer and the model layer one above the bed layer. The fixed value settling velocity hardly allows for vertical SPM variations. The effect on the spatial SPM distribution for the top layer for July 1994 is given in Fig. 13; and (4) the simulations with seasonally reduced erosion (28% lower) both reduce the GoF functional by about 6% relative to the corresponding non-reduced cases. Comparing this with the 2D simulations 9, 11 and 13 (erosion input 50% lower; period March–September), in which the GoF criterion decreased by in total 11%, tentatively confirms that the reactions of the 3D model and the 2D model to reduction in coastal erosion are comparable. It may be expected that

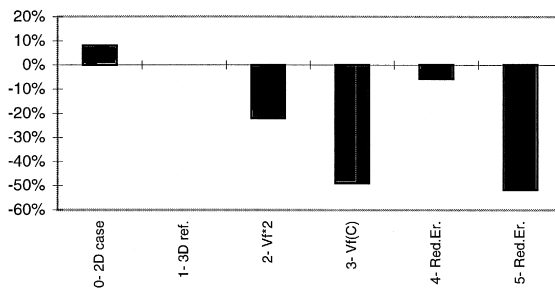


Fig. 10. Change of the GoF criterion in percentage for five sensitivity simulations with the 3D SPM model, relative to a 3D reference simulation (index 1). Simulation period 1st April–1st August 1994.

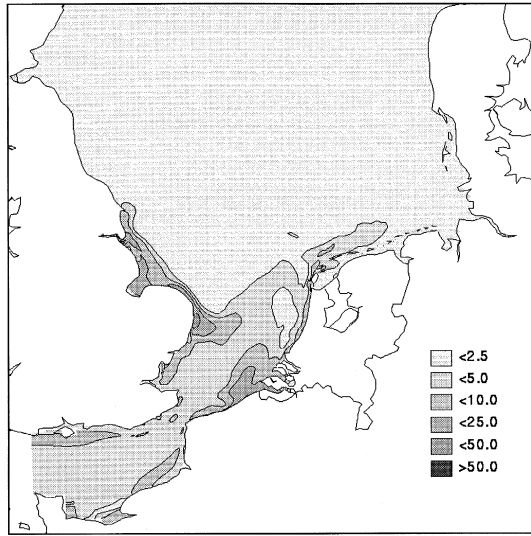


Fig. 11. Spatial distribution of settling velocity  $w_s = \lambda C^m$  ( $\text{m day}^{-1}$ ) of the top layer at 5th July 1994, for  $\lambda = 0.5$  and  $m = 1$ .

this is the case for all dumping and boundary condition variations that are not in stratified areas.

The explicit inclusion of vertical process descriptions clearly gives better modelling results, notably for the coastal zone, where high values and vertically varying concentra-

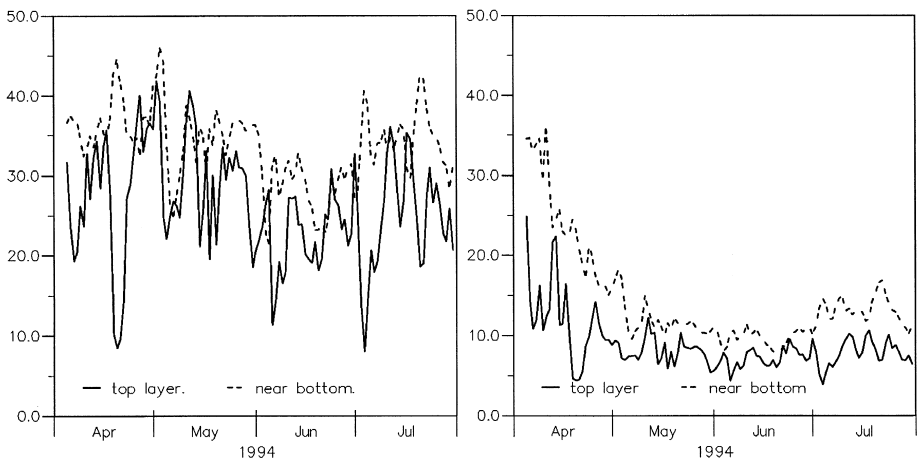


Fig. 12. Time history for daily averaged concentrations at Hoek van Holland in the top layer, and in one layer above the bed layer, for (left frame) model with concentration-independent settling velocity,  $w_s = 5 \text{ m day}^{-1}$  and (right frame) concentration-dependent settling velocity,  $w_s = \lambda C^m$ , with  $\lambda = 0.5 \text{ kg}^{-m} \text{ m}^{3m+1} \text{ day}^{-1}$  and  $m = 1$ .

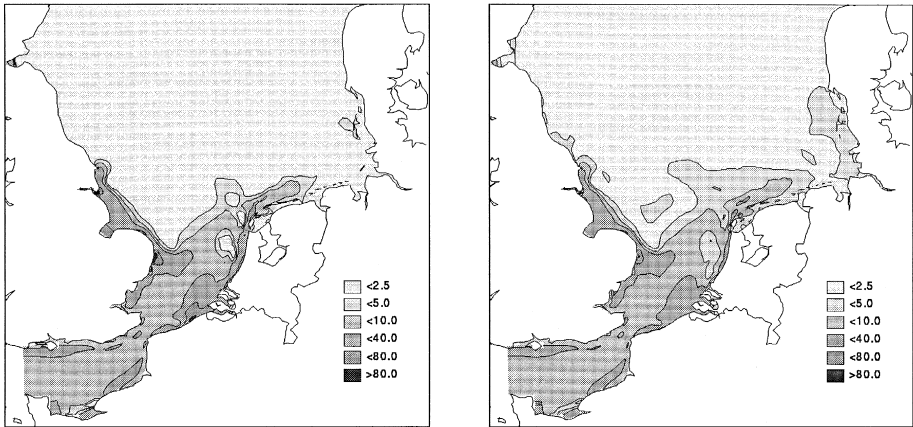


Fig. 13. (Left frame) Surface concentrations of SPM on 5th July 1994 for 3D model with fixed settling velocity,  $w_s = 5 \text{ m day}^{-1}$  and (right frame) with concentration-dependent settling velocity,  $w_s = \lambda C^m$ , with  $\lambda = 0.5 \text{ kg}^{-m} \text{ m}^{3m+1} \text{ day}^{-1}$  and  $m = 1$ .

tions occur and salinity stratification can be important (Rhine outflow). For the stratified region of the Dutch Coast, where strong seasonal variation of suspended sediment is observed, this is a clear necessity. For SPM, the step from 2D modelling to 3D also makes the modelling easier, as the added model parameter has a very pronounced effect on the end result. One may expect that for 3D models that simulate both salinity and temperature, the stratification effect is even more pronounced.

The results with seasonally reduced coastal erosion showed that for non-stratified areas, the results from the 2D model sensitivity analysis may still be expected to be good indicators for what can be expected in 3D models, e.g. what will be its suitable inputs and parameter settings.

For SPM model optimisation or calibration, a two-step approach is therefore suggested: (a) perform a full optimisation of the model in 2D; (b) start the 3D simulations using best estimates for all parameters in 2D and optimise parameters ( $\lambda$  and  $m$  ( $m \geq 1$ )) for the concentration-dependent settling velocity.

## 6. Summary, conclusions and way forward

### 6.1. Objective

The objective of this paper was to review recent progress in the simulation of SPM in the North Sea using sensitivity analyses. It extended the modelling of SPM on the local coastal scale (described in preceding papers) to modelling of SPM on the scale of the North Sea, with a focus on representing SPM patterns and their distribution through the

seasons. Concentrating on larger-scale longer-term motion of silt-sized sediment, the value of both in situ and remotely sensed observations was assessed.

### *6.2. Modelling using in situ data*

The simulations with two 2D rectilinear model versions showed how the extensive in situ data set on SPM acquired in the NSP can be used to identify the sources of sediment and derive a characteristic and meaningful settling velocity. Direct comparison of the results of the multi-regression approach used with in situ observations was hampered by: limited availability of observations, poor time and space resolution and sharp SPM concentration gradients close to the sources (not adequately resolved by the model).

### *6.3. Curvilinear modelling approach*

A boundary curvilinear modelling approach with increased resolution in the coastal zone was introduced to model the large-scale patterns of sediment and their behaviour over time, its local detail in principle resolving the exchange between coastal zone and open North Sea. Hydrodynamic simulations examined the effects of variations in model bathymetry, bed friction and wind forcing formulations. These showed that such variations have a strong effect on the resulting net volume flux through the Dover Strait, consistent with the ranges found in literature on modelling and field data assessments. It may be concluded that the formulation of and model response to varying meteorological forcing is an important topic for further research.

In the sediment transport model, the Krone–Partheniades formulations were used to describe erosion and sedimentation processes. The magnitude of the bed stress involves a superposition of contributions due to both currents and waves. The latter component was estimated by applying a special enhancing technique to large-scale wave model results. A concentration-dependent settling velocity generally used for estuaries was applied.

### *6.4. Sensitivity analysis using NOAA remote sensing data*

A formal GoF approach incorporating a least squares norm was used to compare zonally averaged 2D model results with NOAA image-based surface sediments concentrations in a quantitative and reproducible way. Starting from an SPM model with best estimates for model parameters and inputs, a sensitivity analysis was performed using a 2D approach. The largest sensitivities were shown to occur for variation of the assumed coastal erosion inputs, and the critical erosion parameters. A refinement of the annual coastal inputs by applying a wind stress based intra-annual variation, also improved the results.

The 3D sensitivity analysis focussed on the formulation of the settling velocity, using the upper model layer results for comparison. It was shown that a concentration-depen-

dent settling velocity (linear) gives markedly better results than a fixed value, notably in the coastal zone where salinity stratification may occur. Furthermore, the sensitivity analysis to inputs and horizontal transport performed with the 2D modelling approach tends to remain valid for 3D model applications. It is concluded that for operational modelling and validation, 2D modelling would be a logical first step to a 3D model set-up.

### 6.5. Conclusions

The above structured analysis and quantification of the effects of uncertainties of inputs and sedimentation/erosion parameters using remote sensing-based concentration data has been shown to be feasible and useful. This analysis provides a much better understanding of the (uncertainties in) sediment distribution and budgets on North Sea scale and in the strengths and weaknesses of our modelling capabilities.

We can anticipate that process studies are likely to contribute to improved erosion/deposition algorithms, and model developments will provide enhanced dynamical descriptions. However, accurate overall simulation will remain dependent on some (inverse) process to reduce the uncertainty in the observational data on sediment sources.

### 6.6. Specific modelling uncertainties

The fundamental uncertainties in modelling SPM fluxes arise from: (i) the dominant role of sediment sources, information on which is often incomplete or inaccurate (extent of source material and associated particle type spectra); (ii) relatively simple (bulk) erosion and deposition formulae (especially regarding the influence of flocculation), though in line with the observational information available for their validation; (iii) insufficient information on bed surface sediments (including seasonal variation) available for resuspension. There are further inaccuracies associated with descriptions of tidal, surge and wave dynamics but these are generally relatively well-prescribed. However, the sensitivity of calculated net long-term advective volume fluxes to model characteristics and set-up remains significant. A key item here is the time-integrated response of the horizontal motion to fluctuating meteorological forcing with the general air–sea momentum transfer formulations.

### 6.7. Specific monitoring uncertainties

Available observations suffer from similar fundamental shortcomings, namely: (i) calibration from sensor units to concentration — including sensitivity to particle size spectra in optical and acoustic instruments and to atmospheric corrections and sun angle effects in remote sensing; (ii) unresolved particle-size spectra; (iii) limited spatial and temporal coverage: remote sensing data provide high resolution spatially but for the surface and at low resolution in time, whereas in situ instruments provide high temporal

resolution for the whole water column but only for single-points. Thus, the fundamental difficulties in simulating SPM transports arise from limited descriptions of key inputs and processes (coastal erosion, rates of sediment erosion and deposition) and limited accuracy in the resolution and parameter range of observations. Under these circumstances, simple simulation models are appropriate. However, despite the general incompatibility between resolution provided by observations and that which is now possible in models, the clear association of major SPM events in specific locations with particular dynamical conditions (e.g. wind–wave stirring, major residual flows, stratification, extreme river discharges, etc.) can provide clear support for model refinement.

### *6.8. Key model refinements*

The analysis and intercomparisons described here illustrate the usefulness and often the need, even within the strategy of minimal modelling, for: (i) fine grid resolution in key (coastal) areas; (ii) fully 3D dynamics (reducing empiricism in deposition formulae); (iii) inclusion of wind–wave effects on bed stress (shallow areas).

### *6.9. Future challenges*

The rapid recent developments in modelling of the dynamics of tides, surges and waves have been noted. Generally, the performance of these models is now limited by the provision of related bathymetry, air–sea momentum transfer and, especially, seabed and coastal sediment data. Thus, integrated modelling-monitoring strategies exploiting inverse modelling and assimilation/GoF techniques are likely to be necessary for the foreseeable future. Progress in atmospheric corrections and in improved calibration of remote sensing data is likely both from advances in basic physics, enhanced spectral resolution of sensors and via synergistic usage of in situ sensors. However, the water surface limitation of remote sensing will remain and thus further development of depth profiling and side-sweeping acoustic instrumentation is similarly important. Studies of basic processes in near-full scale of fluxes etc. will continuously enhance our understanding of the relationships between tide- and wave-induced stresses and associated sediment erosion.

## **Acknowledgements**

The present work was funded by the EU MAST III project PROMISE under contract number MAS3-CT950025 and co-funded by WL/Delft Hydraulics' basic research programme. The authors gratefully acknowledge the permission of the Royal Netherlands Meteorological Institute for use of the NOAA/AVHRR data, and that of the Norwegian Meteorological Institute to use their historic wind and pressure data. The authors thank the WASA group and Marek Stawarz of GKSS for making available results of the WASA wave modelling study and Jean-Claude Salomon of IFREMER for

bathymetry data. Last but not least, we thank David Prandle at POL and Gerbrant van Vledder, formerly at Delft Hydraulics, for the constructive discussions on the present work.

## Appendix A. SPM sources and sinks for the North Sea

### A.1. Table A1 Supply of sediments to the North Sea

Process	Location	Reference	SPM supply ( $\times 10^9$ kg year <sup>-1</sup> )
Net inflow through open sea boundaries	Dover Strait	Eisma and Irion (1988)	20–30
		Pohlmann and Puls (1994)	13.6
		McManus and Prandle (1997)	44.4
	Atlantic Ocean And Baltic	Eisma and Irion (1988)	10.5
		Pohlmann and Puls (1994)	13.3
	Total	Eisma and Irion (1988)	30–40
		Pohlmann and Puls (1994)	26.9
McManus and Prandle (1997)		86	
Coastal erosion	Holderness	Odd and Murphy (1992)	2.61
		McCave (1987)	1.4
	Norfolk + Suffolk	Odd and Murphy (1992)	6.27
		McCave (1987)	0.79
	Total	McManus and Prandle (1997)	0.7
		Eisma and Irion (1988)	2.2
Odd and Murphy (1992)		8.88	
River inputs	Total	McCave (1987)	2.5
		Eisma and Irion (1988)	4.8
Bed erosion	Flemish Banks	Boon et al. (1997)	4.41
		van Alphen (1990)	1
	Total	Eisma (1981)	< 2.4
Dumping	Loswal Noord	Eisma and Irion (1988)	9–13.5
		Boon et al. (1997), retention = 0.55	2.36
	Off Zeebrugge	Boon et al. (1997)	4.49
	Thames Entrance	Boon et al. (1997)	0.3
	Humber Entrance	Boon et al. (1997)	3.41
	Other	Boon et al. (1997)	3.5
	Total	Boon et al. (1997)	14
	Primary production	Total	Eisma (1981)
Atmospheric deposition	Total	Eisma (1981)	1
All processes	Total	This table	61–142.6

## A.2. Table A2 Loss of sediments from the North Sea

Process	Location	Reference	SPM supply ( $\times 10^9$ kg year <sup>-1</sup> )
Net outflow through boundaries (loss)	Atlantic Ocean	Eisma and Irion (1988)	-11.4 to -14.3
		Pohlmann and Puls (1994)	-5.2
Sedimentation (loss)	Wash	McCave (1987)	-0.8 to -1.6
		Eisma and Irion (1988)	-2 to -3
		McManus and Prandle (1997)	+3.2 (supply!)
	Wadden Sea	McCave (1987)	-3
		Eisma and Irion (1988)	-2 to -3
	Oyster Ground	Eisma and Irion (1988)	-2
	German Bight	Eisma and Irion (1988)	-3 to -7.5
	Other estuaries	Eisma and Irion (1988)	-1.8
	Outer Silver Pit	Eisma and Irion (1988)	-1 to -4
	Norway, Skagerrak, Kattegat	Eisma and Irion (1988)	-25
	Total		-31.6 to -45.3
Dumping on land	Total	Eisma and Irion (1988)	-2.7
All processes	Total	This table	-45.7 to -62.3

## References

- Amos, C.L., Mosher, D.C., 1985. Erosion and deposition of fine-grained sediments from the Bay of Fundy. *Sedimentology* 32, 815–832.
- Balson, P.S., Laban, C., Schüttenhelm, R.T.E., Paepe, R., Baeteman, C., 1991. Ostend: sheet 52°N/02°E. Sea bed sediments and holocene geology, 1:250000 series British Geological Survey, Geological Survey of the Netherlands and Belgian Geological Survey.
- Baumert, H., Chapalain, G., Smaoui, H., McManus, J.P., Yagi, H., Regener, M., Sündermann, J., Szilagy, B., 2000. Modelling and numerical simulation of turbulence, waves and suspended sediment for pre-operational use in coastal seas. This volume.
- Boon, J.G., Baart, A.C., 1996. Meetstrategie 2000+, Integration of remote sensing, in-situ observations and model simulations of suspended matter in the Dutch coastal zone. Delft Hydraulics Report Z2066 (in Dutch).
- Boon, J., van der Kaaij, T., Vos, R.J., Gerritsen, H., 1997. Modelling of suspended matter (SPM) in the North Sea, model set up and first sensitivity analysis. Delft Hydraulics Research Report Z2025.
- Boxall, S., Cabioch, L., Chabert d'Hieres, G., Collins, M., Guegueniat, P., Salomon, J.C., Staham, P., Waterl, M., 1995. Fluxmanche II hydrodynamics and biogeochemical processes and fluxes in the Channel, MAST 2-CT 94-0089, Second MAST days and EUROMAR market, 7–10 November 1995, Project reports, vol. 1, pp. 121–136.

- British Geological Survey (BGS). Sea bed sediments around the United Kingdom (north and south sheets). Scale 1:1000000.
- Burt, T.N., 1986. Field settling velocities of estuary muds. In: Mehta, A.J. (Ed.), *Estuarine Cohesive Sediment Dynamics*. Lecture Notes on Coastal and Estuarine Studies vol. 14 Springer, Berlin, pp. 126–150.
- Chapalain, G., Thais, L., 2000. Tide, turbulence and suspended sediment modelling in the eastern English Channel. This volume.
- de Kok, J.M., 1992. A three-dimensional finite difference model for computation of near- and far-field transport of suspended matter near a river mouth. *Continental Shelf Research* 12 (5/6), 625–642.
- Delft3D, 1997. Delft 3D-modelling system, User and Reference Manuals. Delft Hydraulics.
- Eisma, D., 1981. The mass balance of suspended matter and associated pollutants in the North Sea. *Rapports et Proces-Verbaux des Reunions — Conseil International pour l'Exploration de la Mer* 181, 7–14.
- Eisma, D., Irlon, G., 1988. Suspended matter and sediment transport. In: Salomons, W., Bayne, B.L., Duursma, E.K., Förstner, U. (Eds.), *Pollution of the North Sea: An Assessment*. Springer, Berlin, pp. 20–35.
- Figge, K., 1981. Karte der Sedimentverteilung in der Deutschen Bucht, Nordsee. Deutsches Hydrographisches Institut, Karte Nr. 2900 (mit beiheft), Hamburg. Area: German Bight, western boundary 6 degrees E, northern boundary 55°05'N. Scale 1:250000. Mercator Projection. Content: grain size distribution of the uppermost 10 cm.
- Geological Survey of the Netherlands, 1986. Raw materials at or near the surface.
- Gerritsen, H., Boon, J.G., van der Kaaij, Th., Vos, R.J., 2000. Integrated modelling of suspended particulate matter in the North Sea. *Estuarine, Coastal and Shelf Science*, submitted for publication.
- Jarke, J., 1956. Der Boden der südlichen Nordsee. Eine neue Bodenkarte der südlichen Nordsee. *Deutsche Hydrographische Zeitschrift* 9, 1–9.
- Johannessen, O.M., Sandven, S., Jenkins, A.D., Durand, D., Petterssen, L.H., Espedal, H., Evensen, G., Hamre, T., 2000. Satellite earth observation in operational oceanography. This volume.
- Jones, J.E., 1999. POL-2G. Proudman Oceanographic Laboratory 2D General Purpose Model. Proudman Oceanographic Laboratory Internal Document No. 131.
- Kappe, B.P., van Koningsbruggen, P., Voogt, L., 1989. Erosion of silt resulting from navigation, extended. Report series Integrated Water Management Ketelmeer. Rijkswaterstaat RIZA, Lelystad, (in Dutch).
- Krone R.B., 1962. Flume studies of the transport of sediment in estuarial shoaling processes, Final report, University of California, Hydraulic Engineering Laboratory and Sanitary Engineering Research Laboratory, Berkeley, CA, USA.
- Lane, A., Riethmüller, R., Herbers, D., Rybczok, P., Günther, H., Baumert, H., 2000. Observational data sets for model development. This volume.
- Lehmann, H.J., Radach, G., Backhaus, J.O., Pohlmann, T., 1995. Simulations of the North Sea circulation, its variability and its implementation as hydrodynamic forcing in ERSEM. *Netherlands Journal of Sea Research* 33, 271–299.
- McCave, I.N., 1987. Fine sediment sources and sinks around the East Anglian Coast (UK). *Journal of the Geological Society (London)* 144, 149–152.
- McManus, J.P., Prandle, D., 1997. Development of a model to reproduce observed suspended sediment distributions in the southern North Sea using Principal Component Analysis and Multiple Linear Regression. *Continental Shelf Research* 17 (7), 761–778.
- Mehta, A.J., 1986. Characterisation of cohesive sediment properties and transport processes in estuaries. *Estuarine Cohesive Sediment Dynamics*. In: Mehta, A.J. (Ed.), *Lecture Notes on Coastal and Estuarine Studies* 14 Springer, Berlin, pp. 290–325.
- Mehta, A.J., Parchure, T.M., Dixit, J.G., Ariathurai, R., 1982. Resuspension potential of deposited cohesive sediment beds. In: Kennedy, V.S. (Ed.), *Estuarine Comparisons*. Academic Press, New York, pp. 591–609.
- Monbaliu, J., Padilla-Hernandez, R., Hargreaves, J.C., Carretero Albiach, J.C., Luo, W., Sclavo, M., Günther, H., 2000. The spectral wave model WAM adapted for applications with high spatial resolution. This volume.
- Monbaliu, J., Hargreaves, J.C., Carretero, J.C., Gerritsen, H., Flather, R., 1999. Wave modelling in the PROMISE project. *Coastal Engineering* 37, 379–407.
- Natural Environment Research Council, 1992. North Sea Project data set. CD ROM, British Oceanographic Data Centre, Proudman Oceanographic Laboratory, UK.

- Nicholson, J., O'Connor, B.A., 1986. Cohesive sediment transport model. *Journal of Hydraulic Engineering* 112 (7), 621–640.
- Odd N.V.M., Murphy, D.G., 1992. Particulate pollutants in the North Sea. Report SR 292, Hydraulics Research, Wallingford.
- Ozer, J., Padilla-Hernández, R., Monbaliu, J., Alvarez Fanjul, E., Carretero Albiach, J.C., Osuna, P., Yu, J.C.S., Wolf, J., 2000. A coupling module for tides, surges and waves. This volume.
- Partheniades E., 1962. A study of erosion and deposition of cohesive soils in salt water, PhD dissertation, University of California, USA.
- Pohlmann, T., Puls, W., 1994. Currents and transport in water. In: Sündermann, J. (Ed.), *Circulation and Contaminant Fluxes in the North Sea*. Springer, Berlin, Section 3.2.
- Prandle, D., 1978. Residual flows and elevations in the Southern North Sea. *Proceedings of the Royal Society London, Series A* 259, 189–228.
- Prandle, D., 1984. A modelling study of the mixing of  $^{137}\text{Cs}$  in the seas of the European continental shelf. *Philosophical Transactions of the Royal Society of London, Series A* 310, 407–436.
- Prandle, D., 1998. Tidal characteristics of suspended sediment concentrations. *Journal of Hydraulic Engineering* 123 (4), 341–350.
- Prandle, D., Ballard, G., Flatt, D., Harrison, A.J., Jones, S.E., Knight, P.J., Loch, S., McManus, J., 1996. Combining modelling and monitoring to determine fluxes of water, dissolved and particulate metals through Dover Strait. *Continental Shelf Research* 16, 237–257.
- Prandle, D., Hydes, D.J., Jarvis, J., McManus, J., 1997. The seasonal cycles of temperature, salinity, nutrients and suspended sediment in the Southern North Sea in 1988 and 1989. *Estuarine, Coastal and Shelf Science* 45, 669–680.
- Prandle, D., Hargreaves, J.C., McManus, J.P., Campbell, A.R., Duwe, K., Lane, A., Mahnke, P., Shimwell, S., Wolf, J., 2000. Tide, wave and suspended sediment modelling on an open coast — Holderness. This volume.
- Puls, W., Kühl, H., Heymann, K., 1988. Settling velocity of mud flocs: results of field measurements in the Elbe and Weser estuary. In: Dronkers, J., van Leussen, W. (Eds.), *Physical Processes in Estuaries*. Springer, Berlin, pp. 404–426.
- Salomon, J.C., Breton, M., 1993. An atlas of long-term currents in the Channel. *Oceanologica Acta* 16 (5–6), 438–439.
- Salomon, J.C., Breton, M., Guegueniat, P., 1993. Computed residual flow through the Dover Strait. *Oceanologica Acta* 16 (5–6), 449–455.
- Salomon, J.C., Breton, M., Guegueniat, P., 1995. A 2D long term advection–dispersion model for the Channel and southern North Sea: Part B. Transit time and transfer function from Cap de La Hague. *Journal of Marine Systems* 6, 515–527.
- Schneggenburger, C., Günther, H., Rosenthal, W., 2000. Spectral wave modelling with non-linear dissipation: validation and application in a coastal tidal environment. This volume.
- Simpson, J.H., Hunter, J.R., 1974. Fronts in the Irish Sea. *Nature* 250, 404–406.
- Sündermann, J. (Ed.), *Circulation and Contaminant Fluxes in the North Sea*, Springer, Berlin.
- ten Brummelhuis P.G.J., Gerritsen, H., van der Kaaij, T., 1997. Sensitivity analysis and calibration of the hydrodynamic PROMISE model using adjoint modelling techniques, Delft Hydraulics Research Report Z2025.
- ten Brummelhuis, P.G.J., Vos, R.J., Gerritsen, H., 2000. Skill assessment of transport models using the adjoint technique. *Estuarine, Coastal and Shelf Science*, submitted for publication.
- Thorn, M.F.C., 1981. Physical processes of siltation in tidal channels. *Proceedings of Hydraulic Modelling applied to Maritime Engineering Problems*. ICE, London, 47–55.
- Uittenbogaard, R.E., van Kester, J.A.Th.M., 1996. Modelling seasonal temperature stratification with TRI-WAQ. Delft Hydraulics Report Z978.
- Uittenbogaard R.E., van Kester, J.A.Th.M., Stelling, G.S., 1992. Implementation of three turbulence models in TRISULA for rectangular horizontal grids. Delft Hydraulics Report Z162.
- Uittenbogaard R.E., Winterwerp, J.C., van Kester, J.A.Th.M., Leepel, H., 1996. 3D Cohesive Sediment Transport parts I and II. Delft Hydraulics Report Z1022.
- van Alphen, J.S.L.J., 1987. Silt occurrence on the Dutch and Belgian continental shelf sections. Rijkswaterstaat, North Sea Directorate, Internal Document Nr. NZ-N-87.09b (in Dutch).

- van Alphen, J.S.L.J., 1990. A mud balance for the Belgian–Dutch coastal waters between 1969 and 1986. *Netherlands Journal of Sea Research* 25, 19–30.
- van Leussen, W., 1994. Estuarine macroflocs and their role in fine-grained sediment transport. PhD Thesis, University of Utrecht.
- van Raaphorst, W., Philippart, C.J.M., Smits, J.P.C., Dijkstra, F.J., Malschaert, J.F.P., 1998. Distribution of suspended particulate matter in the North Sea as inferred from NOAA/AVHRR reflectance images and in situ observations. *Journal of Sea Research* 39, 197–215.
- van Rijn, L.C., 1993. *Principles of Sediment Transport in Rivers, Estuaries and Coastal Seas*. Aqua Publications, Amsterdam.
- van Vledder, G., 1997. Transformation of wave conditions from the WASA grid to the PROMISE grid and their parameterisation in the bed stress. Delft Hydraulics Research Report Z2025.
- Vos R.J., Schuttelaar M., 1995. RESTWAQ, Data assessment, data-model integration and application to the Southern North Sea, BCRS report 95-19, Delft, The Netherlands.
- Vos, R.J., Schuttelaar, M., 1997. An integrated data-model system to support monitoring and assessment of marine systems. In: Stel, J.H. (Ed.), *Proceedings of the First International Conference on EuroGOOS*, Elsevier Oceanography Series 62, The Hague, Netherlands, pp. 507–515.
- Vos, R.J., ten Brummelhuis, P.G.J., Gerritsen, H., 2000. Integrated data-modelling approach for suspended sediment on a regional scale. This volume.
- WASA Group, 1995. The WASA project: changing storm and wave climate in the Northeast Atlantic and adjacent seas. *Proceedings of the 4th International Workshop on Wave Hindcasting and Forecasting*, Banff, Canada.
- Winterwerp, J.C., 1989. Flow-induced erosion of cohesive beds; a literature study. Rijkswaterstaat — Delft Hydraulics Report No. 25.